JOURNAL
OF THE AMERICAN CHEMICAL SOCIETY

VOLUME 101, NUMBER 2 JANUARY 17, 1979

Dynamic and Static Aspects of Solubilization of Neutral Arenes in Ionic Micellar Solutions

Mats Almgren, Franz Grieser,* and J. Kerry Thomas

Contribution from the Radiation Laboratory,‡ University of Notre Dame, Notre Dame, Indiana 46556. *Received July 20, 1978*

Abstract: The kinetics of solubilization and the solubilities of neutral arenes in ionic micellar systems have been measured using phosphorescence, fluorescence, and steady-state absorption techniques. The exit rates for the arenes naphthalene, biphenyl, and 1-methylnaphthalene were measured using their phosphorescence as a monitor, and found to be $>5 \times 10^4\ s^{-1}$. The exit rate of 1-bromonaphthalene, from NaLS micelles, was determined as $2.5 \times 10^4\ s^{-1}$. For this molecule the entrance rate was measured as $5\text{–}8 \times 10^9\ M^{-1}\ s^{-1}$, which can be considered a representative value for other arenes. Distribution constants between arenes and micelles have been measured both at low and saturation probe to micelle ratios. The distribution constants obtained at the different probe to micelle ratios are in approximate agreement, indicating that the arenes are dispersed among the micelles consistent with a Poisson distribution. An empirical model for the solubilization process is presented which incorporates the "site" of solubilization of the arene and the factors which govern the exit and entrance rates from the micelle.

Introduction

It is well known that the solubility of a hydrophobic compound in water can be dramatically enhanced by the addition of a surfactant to the aqueous solution.[1,2] It has also been shown that the enhanced solubilization is largely due to the formation of micelles by the surfactant, because below the critical micelle concentration (cmc) little increase in solubility is observed, yet above the cmc the increase in solubility is directly proportional to the surfactant concentration.

The physical model usually presented[3] to describe the solubilization behavior is one where the additive is either incorporated in the interior of the micelle or attached to its surface, or both.[4] The position of the solubilized additive within the micelle is considered to depend on the relative hydrophobic or hydrophilic nature of the substrate. For example, if the compound has both a polar and hydrophobic end, the polar region will orientate itself toward the head group of the surfactant whereas the other end will become involved with the hydrocarbon "tails" of the micelle interior.

Like the surfactant monomer the solubilized additive is not rigidly fixed in the micelle; not only can it move about within the micelle, but it is also in constant dynamic equilibrium with the bulk aqueous phase.[5,6] For surfactant monomers the dissociation rate constant[7] is of the order of $10^5\text{–}10^9\ s^{-1}$, strongly dependent on the length of the hydrocarbon chain. The association rate constant is near diffusion controlled: $10^8\text{–}10^9\ M^{-1}\ s^{-1}$.[7] If the solubilized compound is a small noncharged species, without the same amphiphilic character as the monomers, the rate constants may be quite different. The dominant factors governing the exit and reentry rates of such species are largely unknown. The entrance rate may of course not be faster than diffusion controlled; if the probe greatly favors the micelles over the aqueous phase it should be expected to remain in the micelle for at least several microseconds.

In this study we have investigated the equilibria between small neutral arenes and various ionic surfactants. The kinetics of exit and reentry are treated quantitatively using phosphorescence as a monitor for the processes occurring in an aqueous micellar solution. Fluorescence quenching results and solubilization data are also presented to expand the results obtained using the phosphorescent probe. The results are instructive in understanding some of the factors which control the exit rate of small neutral molecules solubilized in a micellar phase.

A phenomenological model for the solubilization process is also presented based on the results of this study. The results and the model permit us to draw some conclusions regarding where the solutes are incorporated in the micelles and how they are distributed among the micelles.

Experimental Section

I. Materials. A. Surfactants. For simplification we have used the designation NaC_xS for the sodium alkyl sulfates, where x denotes the length of the alkyl chain; similarly C_xTAB for the alkyltrimethylammonium bromides. Two exceptions are NaLS (sodium lauryl sulfate) and CTAB (cetyltrimethylammonium bromide), because these abbreviations are widely used in the literature. $C_{12}AC$ refers to dodecylammonium chloride.

NaLS (BDH specially pure) was used as supplied. NaLS (Eastman) which had been twice recrystallized from 95% EtOH was also used in preliminary measurements of the phosphorescence study. Results similar to those obtained with the BDH NaLS were also obtained with the recrystallized surfactant. CTAB (Eastman) was twice recrystallized from EtOH–water mixtures. The cmc values for NaLS and CTAB were measured as 8.0×10^{-3} and 8.5×10^{-4} M, respectively, in good agreement with accepted literature values. We have also measured the lifetime of the hydrated electron (a sensitive test

† Department of Physical Chemistry, Chalmers University of Technology, Fack S-402 20, Gothenburg, Sweden.

‡ The research described herein was supported by the Office of Basic Energy Science of the Department of Energy. This is Document No. NDRL-1908 from the Notre Dame Radiation Laboratory.

0002-7863/79/1501-0279$01.00/0

for certain impurities) in solutions containing these surfactants and found the results to be comparable to previous results using extensively purified surfactants. ZnLS was made from NaLS and $ZnSO_4$ by the method described in ref 8. The ZnLS was recrystallized from distilled water; other surfactants were Eastman preparations and used as supplied.

B. Arenes. 1-Bromonaphthalene, 1-methylnaphthalene, biphenyl, anthracene (Eastman Chemical Co.); 4-bromo-*p*-terphenyl (Aldrich); benzene, toluene, *p*-xylene (Fisher Scientific Co.) highest grade available—all these chemicals were used as supplied. Naphthalene (Eastman) was zone refined. Pyrene (Eastman) was purified by thin layer chromatography.

C. Other Chemicals. NaCl (BDH Chemicals Ltd., Aristar), NaBr (Fisher Scientific Co.) research grade, $TlNO_3$ (Ventron) ultrapure, $NaNO_2$ (Fluka) purest grade, and pentanol (Aldrich Chemical Co.) redistilled were used. All samples were prepared with quadruply glass distilled water. The phosphorescence samples were nitrogen saturated using oxygen-free N_2.

II. Phosphorescence Lifetime Measurements. The methods used to prepare the samples before determining their phosphorescence lifetimes have been described elsewhere.[9] The samples were subsequently excited by a 2.5-μs flash from a Xenon Corp. flash lamp assembly (N-723C flash tube, Model 422B micropulser). The emission observed perpendicular to the direction of the flash was passed through a Bausch and Lomb monochromator and detected with a nine-stage 1P28 photomultiplier. The signal was then displayed on a Tektronix 546B storage oscilloscope, and the trace photographed on a 10 000 ASA Polaroid film for analysis.

III. Fluorescence Measurements. A stock solution of naphthalene in water was initially prepared at 10^{-4} M. This was equilibrated for 3 days, then twice filtered through a 0.45-μ Millipore filter. The absorbance reading in water was 0.21 ($\sim 4 \times 10^{-5}$ M). The absorbance of the stock solution was periodically checked and found to be constant. The salt solutions were prepared by using appropriate aliquots (from microliter syringes) of 2 M stock solutions of NaCl and NaBr in 10-mL standard flasks containing a weighed amount of dry surfactant. The flasks were then filled to the mark using stock solutions of naphthalene in water. All emission readings were taken using the same 1-cm quartz cell to maintain as much relative consistency between the measurements as possible. The emission intensities were measured using a Hitachi Perkin-Elmer MPF-44 spectrophotometer and absorption scans were recorded on a Perkin-Elmer Coleman 124 spectrophotometer.

IV. Solubility Measurements. Surfactant solutions were stirred with excess substrate for several days at an elevated temperature, and then allowed to equilibrate at room temperature ($\sim 21 \pm 1$ °C) for several hours. Aliquots from the saturated solution were used in determining the concentration of the solubilized additive. These were first spun in a laboratory centrifuge. Samples of the clear solution were then transferred with care to absorption cells, or, if it was necessary, to volumetric flasks for dilution. The absorbances were measured with a Cary 219 UV/vis spectrophotometer. Absorption measurements of aliquots of the saturated stock solution were again taken several hours after the first measurement to check that the solution had indeed reached saturation.

The procedure was slightly modified in the cases of $NaC_{14}S$ and $NaC_{16}S$. These surfactants have a Krafft point well above room temperature. The centrifugation and absorbance measurements had to be carried out at elevated temperatures to prevent precipitation of the surfactant. The results in these cases are probably overestimated owing to supersaturation of the solutions.

In some cases (pyrene in CTAB, 1-bromonaphthalene, biphenyl, 1-methylnaphthalene in CTAB, and NaLS or $NaC_{14}S$) the substrate phase was clearly changed during the saturation. In the case of pyrene we believe that this was due to attachment of surfactant monomers to the crystal surface. The solubility measurements may be slightly low because of a slight decrease of the surfactant concentration in the solution. For the more soluble substrates—fluid at room temperature—a solid phase was present at saturation. This phase presumably contains both substrate and surfactant, and perhaps water. In any case, the saturation limit in these cases does not represent the equilibrium between micellar solution and pure substrate. That equilibrium may be impossible to establish.

Theory

I. Exit Rates of Solutes from Micelles. The exit rate for a solubilized arene from a micelle can be expected to be relatively slow;[5,6,10] therefore common fluorescence techniques are not useful in studying the exit process. However, emission methods can still be used if the probe is a long-lived phosphorescent molecule.[11] We reported in a previous publication[12] that with due care long lived phosphorescence from aromatic hydrocarbons can be seen in deoxygenated micellar solutions at room temperature. The approach used to utilize the phosphorescent solutes to study the exit and reentry rates between two coexisting phases is described below.

A simple kinetic model for the partitioning of a phosphorescent probe P* between an aqueous phase and micelle (M) is given by

$$\mathrm{MP}^* \underset{k_+}{\overset{k_-}{\rightleftharpoons}} \mathrm{M} + \mathrm{P}^* \tag{1}$$

$$\mathrm{P}^* \xrightarrow{k_\mathrm{P}} h\nu + \mathrm{P} \tag{2}$$

$$\mathrm{MP}^* \xrightarrow{k_\mathrm{MP}} h\nu + \mathrm{MP} \tag{3}$$

Reactions 2 and 3 also include inherent quenching modes other than spontaneous emission; the rate constants k_P and k_MP take this into account. MP* refers to the micelle containing the excited probe, and P* to the excited probe in the aqueous phase of the dynamic system.

If a water-soluble triplet quencher, Q, is added to such a system where

$$\mathrm{P}^* + \mathrm{Q} \xrightarrow{k_\mathrm{q}} \text{quenching} \tag{4}$$

is the only effective quenching reaction of Q, i.e., there is no quenching of the excited probe in the micelle, one would expect a decrease in the observed phosphorescence lifetime with an increase in the quencher concentration until the exit rate becomes the controlling step to the quenching. At this point a further increase in the quencher concentration would not change the observed phosphorescence lifetime.

The kinetic equations which can be constructed from eq 1–4 are as follows:

$$-\frac{\mathrm{d[MP^*]}}{\mathrm{d}t} = k_-[\mathrm{MP^*}] - k_+[\mathrm{M}][\mathrm{P^*}] + k_\mathrm{MP}[\mathrm{MP^*}] \tag{5}$$

$$-\frac{\mathrm{d[P^*]}}{\mathrm{d}t} = k_\mathrm{q}[\mathrm{P^*}][\mathrm{Q}] + k_\mathrm{P}[\mathrm{P^*}] - k_-[\mathrm{MP^*}] + k_+[\mathrm{M}][\mathrm{P^*}] \tag{6}$$

Assuming steady-state conditions for [P*], i.e.

$$-\frac{\mathrm{d[P^*]}}{\mathrm{d}t} \simeq 0$$

then

$$[\mathrm{P^*}] = \frac{k[\mathrm{MP^*}]}{k_\mathrm{q}[\mathrm{Q}] + k_\mathrm{P} + k_+[\mathrm{M}]} \tag{7}$$

Substitute (7) into (5)

$$-\frac{\mathrm{d[MP^*]}}{\mathrm{d}t} = k_-[\mathrm{MP^*}] - \frac{k_+[\mathrm{M}]k_-[\mathrm{MP^*}]}{k_\mathrm{q}[\mathrm{Q}] + k_\mathrm{P} + k_+[\mathrm{M}]} + k_\mathrm{MP}[\mathrm{MP^*}]$$

The disappearance of MP* thus follows first-order kinetics. The observed phosphorescence signal may have contributions from both the micelles and the aqueous phase (although normally the signal from the aqueous phase will be very weak). The contribution from MP* and P* will be proportional to the respective concentrations since [P*] is proportional to [MP*] by eq 7. The observed signal is also proportional to [MP*], and the observed rate constant is given by

$$k_{obsd} = \frac{1}{\tau_{obsd}} = k_- + k_{MP} - \frac{k_- k_+[M]}{k_q[Q] + k_P + k_+[M]} \quad (8)$$

This equation shows that as the quencher concentration increases k_{obsd} approaches a plateau value of $k_- + k_{MP}$. If $k_{MP} \ll k_-$, as is the case with long-lived phosphorescence, the escape rate (k_-) of the probe can be measured.

It is also worth noting at this point that if the conditions are chosen such that $k_+[M]$ is much greater than $k_q[Q] + k_P$, eq 8 can be approximated by

$$k_{obsd} = \frac{(k_- k_q + k_{MP} k_q)[Q]}{k_+[M]} + \alpha \quad (9)$$

If k_- is greater than k_{MP}, this equation can be further reduced to

$$k_{obsd} = \frac{k_- k_q[Q]}{k_+[M]} + \alpha \quad (9a)$$

where

$$\alpha = \frac{k_P k_- + k_{MP} k_P + k_{MP} k_+[M]}{k_+[M]}$$

The usefulness of eq 9 lies in the region where the exit rate k_- cannot be found because it is beyond the time resolution of the equipment. The equilibrium constant can still be found from the slope of k_{obsd} vs. [Q] provided that k_q and [M] are known.

To apply these kinetic equalities (eq 8 and 9) a number of experimental conditions must be satisfied.

(1) The probe molecule must be far more soluble in the micelle phase than in the water phase such that [MP*] $\gg$ [P*] is true. It furnishes the situation which allows the application of the steady-state approximation.

(2) The quencher must only act in the bulk aqueous phase. If the quencher was capable of quenching at the micelle surface, deactivation of the excited probe would occur without the necessity of the probe exiting.

(3) The concentration of the probe is low such that self-quenching of the excited state is unimportant. This condition is easily controlled by choosing a concentration ratio of probe to micelle which minimizes multiple occupancy of a micelle.

With these conditions enforced, eq 8 should describe the observed behavior of the emission decay rate constant with dependence on both the micelle concentration and quencher concentrations. As mentioned earlier, this relationship shows that as the quencher concentration is increased, k_{obsd} will approach a limiting value equal to $k_- + k_{MP}$. If the exit rate is faster than the inherent lifetime of the probe in the micelle (k_{MP}), the limiting value is a measure of the exit time (k_-). Provided that k_q and k_P are known, then k_+, the reentry rate constant, can be calculated at a known quencher and micelle concentration (see eq 8).

The systems used in this study are presented in the Results section.

II. Micelle–Solute Equilibrium Association Constants. In a recent publication by Quina and Toscano[13] a fluorescence quenching method was described to measure the equilibrium constant between a micelle and a solubilized additive. In their case the probe was a fluorescent molecule, and quenching effects were attributed to the probe in free solution on a time scale where escaping probes would not interfere with simple free solution kinetics. They showed that the relationship

$$\frac{\phi_f^\circ}{\phi_f^\circ - \phi_f} = \left|\frac{a\phi^\circ_{fm}}{b\phi^\circ_{fw}} + 1\right| \left|1 + \frac{1}{k_q \tau^\circ_{fw}[Q]}\right| \quad (10)$$

relates the change in the relative quantum yield of fluorescence ϕ_f in the presence of the bulk solution quencher Q, provided that the absorptivity of the probe is the same in both phases. $k_q\tau^\circ_{fw}$ is the Stern–Volmer quenching constant, ϕ_f° is the total fluorescence yield in the absence of a quencher, ϕ°_{fm} and ϕ°_{fw} are the fluorescence quantum yields in the micelle and water phases, respectively, and a and b are the fraction of probe in the micelle and water, respectively. The ratio of a/b that can be derived from this equation is related to the equilibrium constant, K_{eq}, for the association of the probe with the micelle by

$$K_{eq} = \frac{k_+}{k_-} = \frac{a}{b}[M]^{-1} \quad (11)$$

Quina and Toscano[13] used the concentration of empty micelles for [M] in eq 11. This implies that only one probe may be incorporated in a micelle. If we instead assume a Poisson distribution of the probes among the micelles, [M] should represent the total concentration of micelles. At occupancy numbers much less than unity the difference is unimportant.

An alternative method of measuring the distribution between the water and the micelle phases is to utilize a feature of the micelle itself. Under certain conditions, the lifetime of the fluorescent probe in water is quite different than that in the micelle. For example, naphthalene fluorescence is quenched by bromide,[14] so if it is incorporated in a CTAB micelle one observes a decrease in the total emission yield compared to that in water. By changing the proportions of dissolved to "free" solute the equilibrium ratio can be obtained from the relationship

$$\frac{I_\infty - I_0}{I_f - I_0} = 1 + (K_{eq}[M])^{-1} \quad (12)$$

I_∞, I_0, and I_f are the relative emission intensity readings at ~100% solubilization, without surfactant present, and at intermediate amounts of surfactant, respectively. This method has also been used, where possible, to compare with the association constants obtained by other methods.

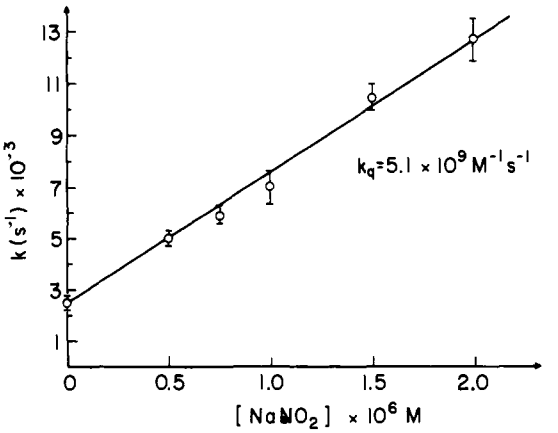

Figure 1. Phosphorescence decay rate of 1-bromonaphthalene in water as a function of $NaNO_2$ concentration.

Results

A. Phosphorescence Quenching Studies. The surfactant chosen for this study was NaLS. It is known to form anionic micelles with an aggregation number (N) of 62 units per micelle.[3] The probe used was 1-bromonaphthalene, which has a relatively strong phosphorescence emission in deoxygenated micellar solution. Since the micelle surface is negatively charged, the water-soluble quencher chosen was NO_2^-. This has a triplet energy of ~53 kcal,[15] and efficiently quenches the triplet state of 1-bromonaphthalene with a rate constant in water of 5×10^9 M^{-1} s^{-1} (see Figure 1). Also, the negatively charged ion ensures that close approach to the micelle surface is minimized so that quenching would be predominantly in the bulk aqueous phase. The effectiveness of reducing the

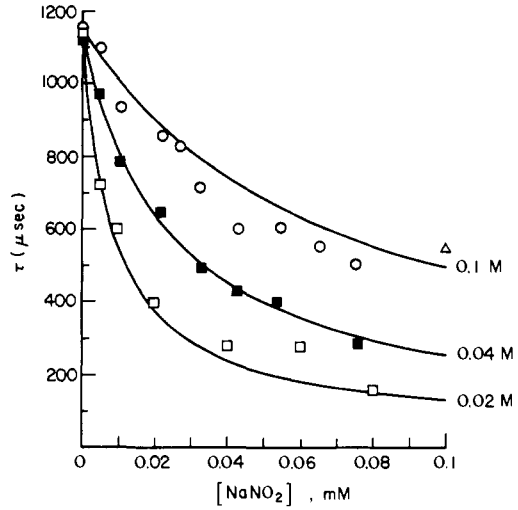

Figure 2. Phosphorescence lifetime of 1-bromonaphthalene as a function of [NaLS] and [$NaNO_2$]. The solid curves are computer "fits" (see text). The parameters used were $k_+ = 7 \times 10^9\ M^{-1}\ s^{-1}$, $k_- = 2.5 \times 10^4\ s^{-1}$, $k_q = 5 \times 10^9\ M^{-1}\ s^{-1}$, $k_p = 2.5 \times 10^3\ s^{-1}$, $k_{MP} = 8.7 \times 10^2\ s^{-1}$, and $N = 62$. The concentration of 1-bromonaphthalene was $\sim 10^{-4}$ M in 0.1 and 0.04 M NaLS, and $\sim 5 \times 10^{-5}$ M in 0.02 M NaLS. The point, Δ, is from the 0.1 M NaLS data given in Figure 3.

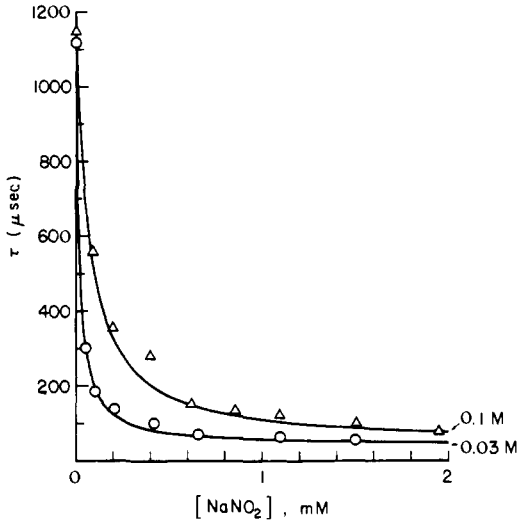

Figure 3. Phosphorescence lifetime of 1-bromonaphthalene as a function of [NaLS] and [$NaNO_2$]. The solid curves are computer "fits" using the same parameters as in Figure 2.

quenching ability of an ion at the surface of like-charged micelles has been shown by others.[6,14]

The lifetime of triplet 1-bromonaphthalene in the water used in these experiments was measured to be $\tau = 400 \pm 20\ \mu s$ ($k_P = 2.5 \times 10^4\ s^{-1}$). The emission intensity was weak and, compared to the signal observed from micellar solubilized 1-bromonaphthalene, imperceptible.

The results shown in Figures 2 and 3 indicate the effects of quencher concentrations and surfactant concentrations on the phosphorescence lifetime. The results obtained for the 0.02 M NaLS system used a 5×10^{-5} M concentration of 1-bromonaphthalene. This was to ensure that the probe/micelle ratio was low such that possible anomalous effects due to multiple occupancy were minimized. The solid lines are from computer simulation curves based on eq 8. This will be discussed in greater detail later.

The surfactant concentrations chosen were all above the cmc.[16] Thus the trend of a decrease in the emission lifetime at a particular quencher concentration as the micelle concentration is decreased can be understood in terms of the model described earlier. Since reentry

$$M + P^* \xrightarrow{k_+} MP^*$$

is in competition with quenching (reaction 4), at a particular quencher concentration more excited probe molecules will reenter a micelle as the micelle concentration is increased. Thus by increasing the average time spent in the protection of the micelles a lengthening of the lifetime of the excited probe is observed.

Figure 3 shows the approach to a limiting value at higher quencher concentrations of $\sim 40\ \mu s$ ($2.5 \times 10^4\ s^{-1}$). In accord with the model this is equal to $\sim k_- + k_{MP}$; since k_{MP} (equal to the reciprocal of the intercept value at zero quencher concentration) is considerably smaller than k_-, the exit rate constant is given by this plateau value.

Having obtained this exit rate constant and together with the other data presented above, the reentry rate constant was calculated from eq 8. Using different quencher concentrations and different micelle concentrations, k_+ was calculated to be in the range $5\text{–}8 \times 10^9\ M^{-1}\ s^{-1}$. Thus the equilibrium value of

$$K_{eq} = \frac{k_+}{k_-} = \frac{[MP]}{[M][P]} = 2\text{–}3 \times 10^5\ M^{-1}$$

is obtained for 1-bromonaphthalene in NaLS. Note that the point made earlier that [MP] ≫ [P] is reflected in this value.

The simulation curves shown in Figures 2 and 3 have been calculated using eq 8. The parameter values used are indicated in the figure captions. As can be seen, a reasonable fit to the experimental data can be obtained in most regions of the quenching range.

Phosphorescence quenching experiments were also conducted at NaLS concentrations in the range 0.2–0.6 M. At these concentrations the solutions were noticeably viscous. The quenching curve at 0.3 M NaLS was the same as that measured for 0.1 M NaLS. At higher surfactant concentrations the quenching curves were reduced below the 0.1 M data.

In particular, the phosphorescence lifetime without added quencher, which increases slightly up to 0.1 M NaLS, decreases markedly at the higher concentrations. This indicates the presence of a quenching impurity in the surfactant preparation. Simultaneously two other effects become operative at these high concentrations. One is that the micelles occupy a considerable portion of the solution volume. As well as this, the negatively charged quencher will be excluded not only from the volume occupied by the micelles, but also by the electrostatic repulsion of the micelle surface, from a region around the micelles. If we consider a NaLS micelle with a radius of 16 Å, and assume that the NO_2^- is in effect excluded from a volume extending, say 15 Å further from the surface (the Debye length at the ionic strength of the curve is about 35 Å), the excluded volume in 0.1 M NaLS amounts to about 12% of the total solution volume. The concentration of a quencher in the water phase is thus higher than the analytical concentration by a factor of 1/0.88.

At high micelle concentrations there is also a change in the size and shape of the micelles.[17] This may have several consequences regarding the quenching behavior. Such effects at high surfactant concentrations make the analyses of the phosphorescence quenching curves difficult. Hence we have restricted our studies to surfactant concentrations of ≤0.1 M.

The effect of various additives on the quenching behavior of NO_2^- was also studied. Figure 4 shows the results of increasing the ionic strength of the solution by the addition of

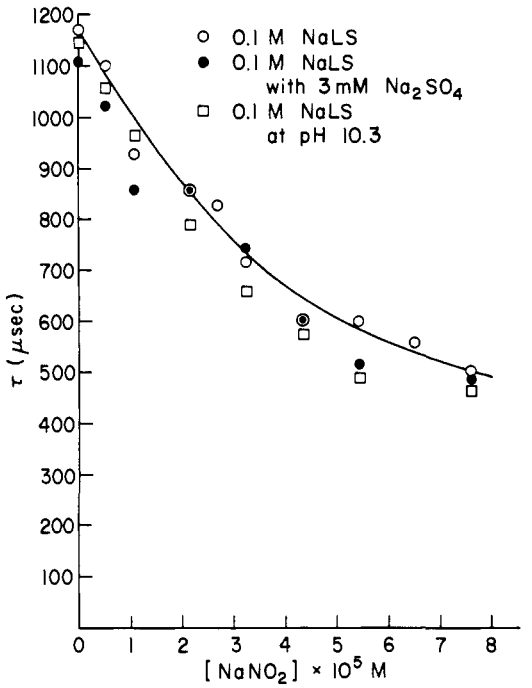

Figure 4. The phosphorescence lifetime of 1-bromonaphthalene in 0.1 M NaLS as a function of $[NaNO_2]$, and in the presence of 3 mM Na_2SO_4, at pH 10.3.

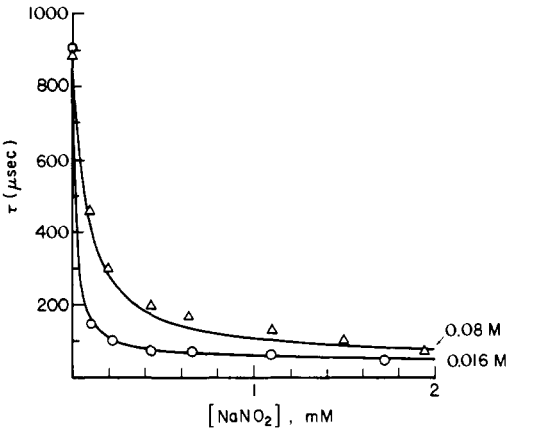

Figure 5. Phosphorescence lifetime of 1-bromonaphthalene as a function of $[NaC_{14}S]$ and $[NaNO_2]$. The solid curves are computer "fits" using the parameters $k_+ = 8 \times 10^9$ M^{-1} s^{-1}, $k_- = 2.2 \times 10^4$ s^{-1}, $k_q = 5 \times 10^9$ M^{-1} s^{-1}, $k_p = 2.5 \times 10^3$ s^{-1}, $k_{MP} = 1.1 \times 10^3$ s^{-1}, and $N = 80$.

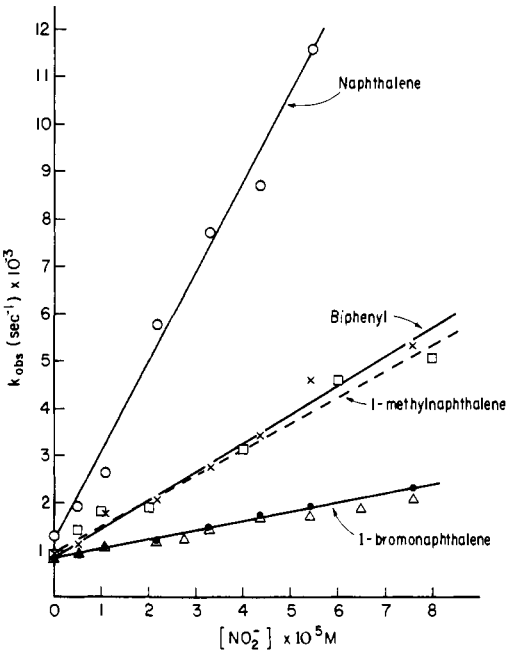

Figure 6. The phosphorescence quenching rate of (1) 1-bromonaphthalene, (2) 1-methylnaphthalene, (3) biphenyl, and (4) naphthalene in 0.1 M NaLS with 3 mM $TlNO_3$, as a function of $[NaNO_2]$. The points, Δ, for 1-bromonaphthalene are without $TlNO_3$ added. Probe concentrations were all ~10^{-4} M.

3 mM Na_2SO_4 and the effect of increasing the pH on the quenching rate. The region of quenching shown is the most sensitive in detecting any change in the entrance or exit rate of the probe. The purpose of adding Na_2SO_4 was primarily to see if the quenching rate of NO_2^- is increased by reducing the repulsion effect of the micellar Stern layer. For similar reasons the pH was changed to 10.3. At normal working conditions the pH of the solution was ~6; however, there is a pH gradient at the micelle surface[18] which makes the pH near the surface considerably less than this value. One possible solution interaction with NO_2^- is the formation of HNO_2 ($pK = 3.37$),[19] a neutral entity conceivably capable of quenching in the micelle. If this did occur the higher pH solution would minimize the formation of HNO_2 and consequently decrease the quenching effect of the added NO_2^-.

As can be seen in Figure 4, within experimental error the additives do not influence the NO_2^- quencher rate and therefore indicate that the latter effects are not responsible for the observed quenching behavior.

A cosurfactant, pentanol, was also added to 0.1 M NaLS solutions to see if the exchange kinetics of the probe were affected. Up to 0.1 M pentanol was added but no noticeable effect on the phosphorescence quenching curve was observed. Essentially, the same curve as shown in Figure 3 for 0.1 M NaLS was obtained.

Using $NaC_{14}S$ as the surfactant the phosphorescence quenching curves obtained are shown in Figure 5. The solid lines are computer curves using eq 8. The best "fit" was obtained with an exit value of 45 μs and an entrance rate of 8×10^9 M^{-1} s^{-1}. The micelle concentration was calculated using an aggregation number of 80 (reported in ref 7). The values obtained for the exit and reentry rates are not significantly different from those of NaLS, and within experimental error can be considered the same. Thus a small change in the micelle size does not appear to influence the equilibrium dynamics to any noticeable extent.

Other molecules studied besides 1-bromonaphthalene had faster micelle exit times and were beyond the time resolution of the equipment (~20 μs). However, the initial decrease in the emission lifetime at lower quencher concentrations ($<10^{-4}$ M) could be obtained and treated as per eq 9. Figure 6 shows the quenching of 1-bromonaphthalene, 1-methylnaphthalene, biphenyl, and naphthalene by NO_2^-. All the solutions included 3 mM Tl^+, which in the case of biphenyl, 1-methylnaphthalene, and naphthalene enhanced the yield of phosphorescence. The curve for 1-bromonaphthalene with and without Tl^+ present is included to show that the steepness of the curves is not a function of the Tl^+. Although the yield of phosphorescence is increased for the biphenyl and naphthalene systems, no such increase is observed in the case of 1-bromonaphthalene. In a previous publication[9] it was shown that the Tl^+ acts as a intermolecular heavy atom which enhances the phosphorescence emission rate of a number of arenes probably in the same manner that a halogen atom acts in an intramolecular perturbation.

The curves show that the plot of k_{obsd} vs. [Q] are linear as

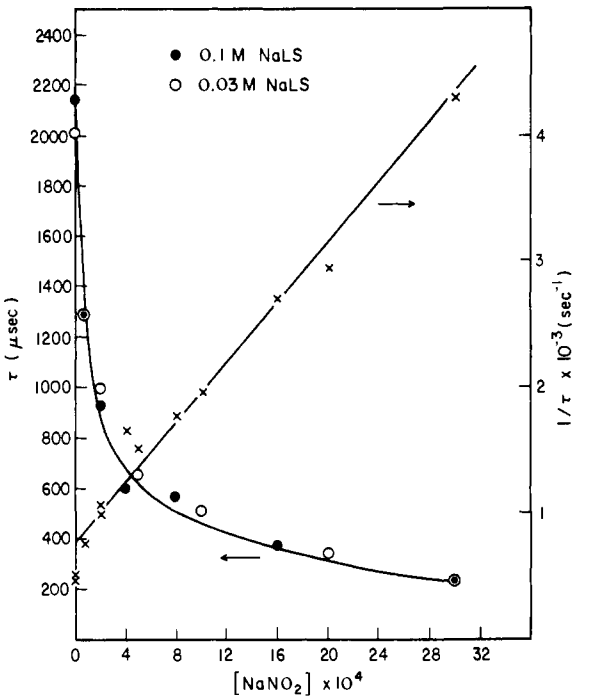

Figure 7. Phosphorescence lifetime and reciprocal lifetime of 4-bromo-*p*-terphenyl in micellar solution as a function of [NaLS] and [$NaNO_2$].

predicted by eq 9 owing to the condition $k_+[M] \gg k_q[Q]$. Relating the slopes of these plots to eq 9, the equilibrium constants for 1-bromonaphthalene can be calculated since both k_2 and [M] are known. The value obtained is 1.8×10^5 M^{-1}, which is in reasonable agreement with the value given earlier. Using the rate constants obtained for this system, the α intercept gives a value of 877, which compares favorably with the observed value of 870. In the case of biphenyl and naphthalene the triplet quenching rate constant k_q using NO_2^- could not be measured. However, considering the results of the study by Treinin and Hayon[15] it is reasonable to say that k_q in these cases is similar to that measured for other naphthalene derivatives, i.e., $2\text{-}5 \times 10^9$ M^{-1} s^{-1}. With this assumption the equilibrium constants for naphthalene, 1-methylnaphthalene, and biphenyl in NaLS can be calculated; the values obtained are given below

arene	slope × 10^{-7} M^{-1} s^{-1}	$K_{eq} \times 10^{-4}$, M^{-1}
1-bromonaphthalene	1.8	18
1-methylnaphthalene	5.9	2.5-5.5
naphthalene	19	0.7-1.7
biphenyl	6.0	2.2-5.4

One other molecule studied was 4-bromo-*p*-terphenyl, which has an emission maximum at about 500 nm in a deoxygenated micellar solution. The phosphorescence quenching curves obtained are shown in Figure 7. As can be seen the phosphorescence lifetime at a particular concentration of $NaNO_2$ does not vary with the micelle concentration. This result can be interpreted as a case where the exit rate of the solubilized arene is slower than the quenching rate of NO_2^- at the "surface" of the micelle. Plotting the data as $1/\tau$ vs. [$NaNO_2$] a linear plot is obtained with a second-order rate constant of 1.2×10^6 M^{-1} s^{-1} (cf. 2.6×10^6 M^{-1} s^{-1} for I^- quenching of singlet biphenyl in NaLS, ref 6). Although an exit rate could not be measured, it must be less than 1.3 ms (7.7×10^2 s^{-1}) to be consistent with the data in Figure 7.

It may be expected that the "surface" quenching rate of NO_2^- for the other arenes studied is similar to that of 4-bromo-*p*-terphenyl; therefore the other quenching curves obtained are true indicators of the equilibrium dynamics. Other information to support this conclusion is seen in the case of 1-bromonaphthalene in NaLS and $NaC_{14}S$. At the higher end of the quencher concentration, the lifetime of the phosphorescence is still different in the two surfactant concentrations. This would not be the case if "surface" quenching were the dominant factor in determining the phosphorescence lifetime, as is illustrated by the data for 4-bromo-*p*-terphenyl.

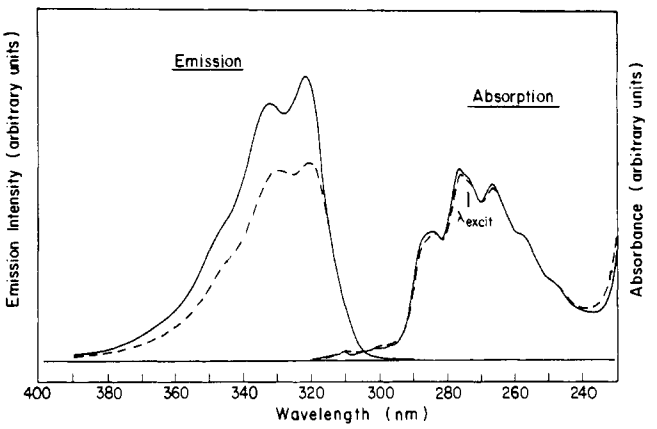

Figure 8. The emission and absorption spectra of naphthalene in aqueous 0.1 M NaCl (dashed curve) and in the presence of 0.09 M NaLS (full curve) (NaCl added to give [Na^+] = 0.1 M). The concentration of naphthalene was $\sim 4 \times 10^{-5}$ M.

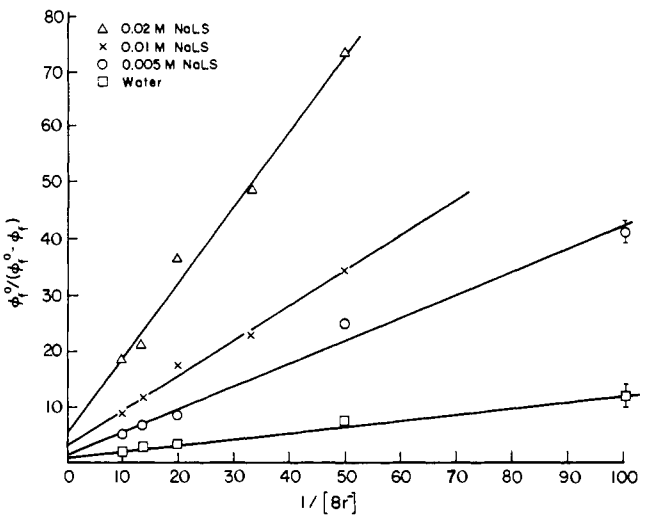

Figure 9. Naphthalene fluorescence quenching by Br^-, plotted in the form given by eq 10. In all cases the [Na^+] equaled 0.1 M, by appropriate additions of NaCl.

B. Fluorescence Quenching Studies. To measure the association constant of naphthalene with NaLS, conditions were chosen similar to those reported by Quina and Toscano.[13] The total free Na^+ ion concentration (cmc + added electrolyte) was maintained at 0.1 M, which gives an aggregation number, N, of 88 (see ref 13). The fluorescence and absorption spectra of naphthalene both in water and in the micellar solution are shown in Figure 8. The spectra show that there is a higher fluorescence yield in the micelle phase than in water. The ratio of $\phi^\circ_{fm}/\phi^\circ_{fw}$ was measured to be 1.52 ± 0.04. The effect of Br^- on the fluorescence yield is shown in Figure 9. The Stern-Volmer quenching constant of naphthalene by Br^- was measured as 9.5 M^{-1} (cf. 8.3 M^{-1}, ref 14. The data permits the calculation of K_{eq} based on eq 10 and 11; the results are presented in Table I. It is also possible to obtain the ratio of a/b from the intercept; however, the accuracy of this value is quite

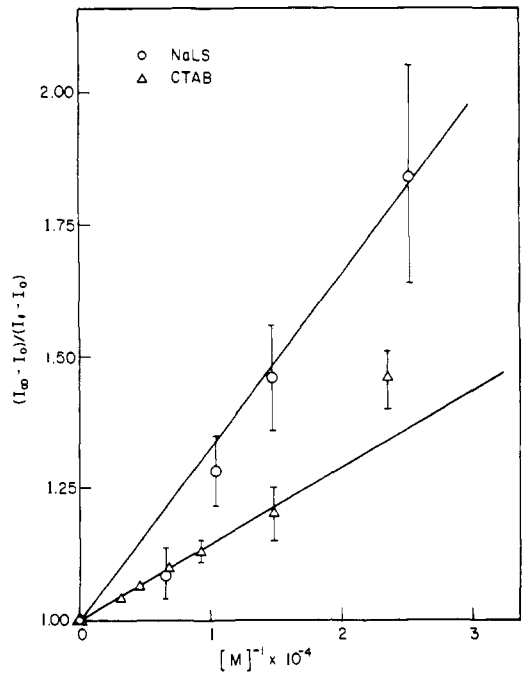

Figure 10. Data for the partitioning of naphthalene in CTAB and NaLS (with 0.1 M Na^+), plotted according to eq 12. Emission intensity readings were taken at the maxima of the spectra shown in Figures 8 and 11.

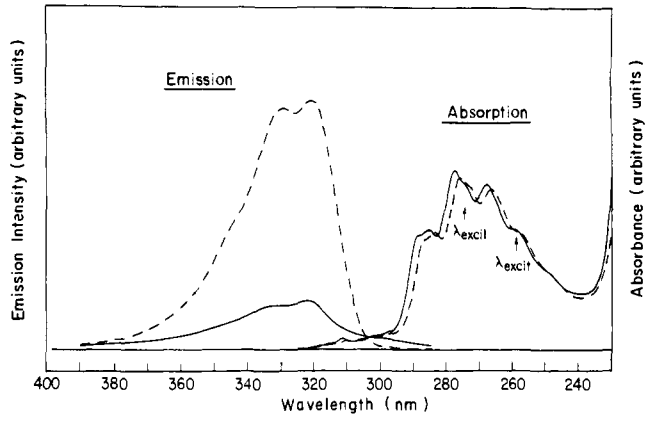

Figure 11. Absorption and emission spectra of naphthalene in water (dashed curve) and 0.05 M CTAB (full curve). Arrows indicate the isosbestic points used to excite the naphthalene to obtain the data given in Figure 10. The concentration of naphthalene was $\sim 4 \times 10^{-5}$ M.

Table I. Distribution Constant for Naphthalene in NaLS and 0.1 M Na^+, Determined by Fluorescence Quenching with Br^-

[NaLS], M	a/b (intercept)	K_{cq} (intercept), M^{-1}	a/b (slope)	K_{eq} (slope) M^{-1}
0.005	1.5	3.8×10^4	2	4.7×10^4
0.01	3.2	3.3×10^4	3.7	3.5×10^4
0.02	5.5	2.6×10^4	8.2	3.9×10^4
av. value		$3.2 \pm 0.6 \times 10^4$		$4.0 \pm 0.7 \times 10^4$

dependent on the line of best fit. Consequently the error limits given in Table I are underestimated.

The partitioning of naphthalene in NaLS and CTAB using the second fluorescence technique described earlier is shown in Figure 10. Unlike NaLS, CTAB does interact with naphthalene; see Figure 11. Therefore the choice of excitation wavelength to ensure equal absorptivity in the aqueous and micellar phases was made at the isosbestic points, 274.5 and 258.5 nm, indicated by the arrows in Figure 11. The data in Figure 10 are the average of three separate determinations. Based on eq 12, the equilibrium constant for naphthalene in NaLS is $3.0 \pm 0.5 \times 10^4$ M^{-1}. That for naphthalene in CTAB using 60 as the aggregation number is $7.0 \pm 0.2 \times 10^4$ M^{-1}. The equilibrium constant for naphthalene in NaLS without the presence of salt could not be determined accurately because of the limited range of micelle concentrations that could be used. The value of K_{eq}/N for naphthalene in ZnLS was determined to be 2.8×10^2 M^{-1}. The aggregation number for this surfactant is not well established, but probably lies in the region of 70–100. Therefore, the K_{eq} of naphthalene with ZnLS is in the range $2\text{–}2.8 \times 10^4$ M^{-1}. A list of all the association constants with comparisons found in the literature is tabulated in Table II.

Table II. Arene/Micelle Distribution Constants Obtained from Kinetic Techniques

arene	surfactant	technique	K_{eq}, M^{-1}
1-bromonaphthalene	NaLS	phosph	$2\text{–}3 \times 10^5$
	$NaC_{14}S$	phosph	$\sim 3.6 \times 10^5$
naphthalene (0.1 M Na^+)	NaLS	fluores	$3.0 \pm 0.5 \times 10^4$
(0.1 M Na^+)	NaLS	Br^- fluores quenching	$4 \pm 1 \times 10^4$
naphthalene	NaLS	phosph	$0.7\text{–}1.7 \times 10^4$
	CTAB[a]	single photon counting	6×10^4
	CTAB	fluores	$7.0 \pm 0.2 \times 10^4$
	ZnLS	fluores	$2\text{–}2.8 \times 10^4$
biphenyl	NaLS	phosph	$2.2\text{–}5.4 \times 10^4$
1-methylnaphthalene	NaLS	phosph	$2.5\text{–}5.5 \times 10^4$

[a] Reference 14.

C. Solubility Measurements. The solubility of various arenes in water and in various ionic micellar solutions is summarized in Table III.

Generally the saturation concentrations in water were calculated using absorption coefficients (ϵ) of the arenes determined in ethanol/water (20–100% ethanol) mixtures. Within experimental error there was no change in ϵ as the solvent composition was changed.

It was also found that the maximum reading of a particular arene absorption band measured in a saturated water solution normally showed little intensity variation when a surfactant was added, although in some cases there was a wavelength shift of the absorption maximum. Thus the maximum additive concentration in the surfactant solution was calculated using the same ϵ as that determined in water.

Exceptions to this procedure were made for the compounds benzene, toluene, *p*-xylene, and pyrene. These arenes did show a significant difference in their absorption coefficients in water, in EtOH, and in the micelle phase. Therefore $\epsilon_{\lambda_{max}}$ was determined in an NaLS micelle solution as 175 (254 nm), 230 (261 nm), and 560 (267 nm) M^{-1} cm^{-1} for benzene, toluene, and *p*-xylene, respectively (cf. ϵ_{water} 130, 224, and 455 M^{-1} cm^{-1}, ref 26). Pyrene is CTAB gave ϵ 40 200 M^{-1} cm^{-1} (337 nm), as compared to ϵ 49 500 M^{-1} cm^{-1} (334 nm) in ethanol and ϵ 29 500 M^{-1} cm^{-1} (334 nm) in water. For these compounds the water solubilities were taken from the literature and listed in Table III.

The distribution constant for 4-bromo-*p*-terphenyl can only be estimated since the solubility of this compound in water could not be directly measured. In 0.05 M NaLS the solubility was 4.2×10^{-6} M (using $\epsilon_{\lambda_{max}}$ 36 000 M^{-1} cm^{-1} at 280 nm determined in ethanol), which gives $\bar{n}_{max} = 0.006$. Since the solubility in water appears to follow the value of $\bar{n}_{max}$ (see

Table III. Solubility Data for Arenes in Micellar Solution (21 ± 1 °C)

	solubility,[a] M	$\bar{n}$[b]	minimum[c] fraction at surface	K,[b] M^{-1}
	Pyrene			
H_2O	6×10^{-7}[g]			
hexane	7.1×10^{-2}			
dodecane	7.4×10^{-2}			
$NaC_{10}S$ (0.08 M)	4.0×10^{-2}	0.4		6.7×10^5
$C_{10}TAB$ (0.09 M)	8.2×10^{-2}	0.8	0.15	13×10^5
NaLS (0.06–0.04 M)	7.0×10^{-2}	1.0		17×10^5
$C_{12}TAB$ (0.04 M)	22×10^{-2}	2.4	0.67	40×10^5
$C_{12}AC$ (0.04 M)	17×10^{-2}	3.8	0.57	63×10^5
$NaC_{14}S$[d] (0.04 M)	10.5×10^{-2}	2.2	0.30	37×10^5
$NaC_{16}S$[d] (0.04 M)	10.9×10^{-2}	3.2	0.33	53×10^5
CTAB (0.04 M)	41×10^{-2}	7.3	0.82	102×10^5
	4-Bromo-*p*-terphenyl			
H_2O	$<10^{-9}$			
NaLS (0.05 M)	4.2×10^{-4}	0.006		$>6 \times 10^6$
	Perylene[e]			
H_2O	$\sim 1.6 \times 10^{-9}$[f]			
NaLS (0.01 M)	1.9×10^{-3}	0.027		1.7×10^7
CTAB (0.01 M)	2.4×10^{-3}	0.043		2.7×10^7
	Anthracene			
H_2O	2.2×10^{-7}[g]			
hexane	1.4×10^{-2}[h]			
NaLS (0.02 M)	0.63×10^{-2}	0.09		4×10^5
CTAB (0.02 M)	3.3×10^{-2}	0.58	0.6	26×10^5
	Naphthalene			
H_2O	2.2×10^{-4}[g]			
hexane	0.91[h]			
NaLS (0.04 M)	0.38	5.4		2.5×10^4
NaLS (0.04 M, 0.1 M NaCl)	0.36	7.1		3.6×10^4
CTAB (0.02 M)	1.11	20.0	0.2	9.1×10^4
	1-Methylnaphthalene			
H_2O	2.1×10^{-4}			
NaLS (0.025 M)	1.06	15		7.1×10^4
	1-Bromonaphthalene			
H_2O	4.5×10^{-5}			
NaLS (0.05 M)	0.66	9.4		2.1×10^5
CTAB (0.05 M)	4.3	76		1.7×10^6
$NaC_{14}S$ (0.025 M)	0.94	19.5		4.3×10^5
	Biphenyl			
H_2O	4.1×10^{-5}			
dodecane	0.72			
NaLS (0.05 M)	0.21	3		7.3×10^4
CTAB (0.05 M)	1.00	17.7	0.28	4.3×10^5
	Benzene			
H_2O	2.3×10^{-2}[i]			
NaLS (0.05 M)	2.5	35		1.6×10^3
CTAB (0.05 M)	12.3	215		9.3×10^3
	Toluene			
H_2O	6.8×10^{-3}[i]			
NaLS (0.05 M)	2.5	35		5.3×10^3
	p-Xylene			
H_2O	1.84×10^{-3}[i]			
NaLS (0.05 M)	2.1	30		1.6×10^4

[a] The solubilities in the micelles have been calculated from $([P]_{tot} - [P]_{aq,sat})/\{([surf] - cmc)V_{hc}\}$ where V_{hc} is the molar volume of the hydrocarbon from which the tail of the surfactant is derived. [b] The aggregation numbers used were 50 ($NaC_{10}S$),[3] 48 ($C_{10}TAB$),[3] 62 (NaLS),[3] (100 ($C_{12}AC$),[20] 50 ($C_{12}TAB$),[3] 80 ($NaC_{14}S$),[7] 100 ($NaC_{16}S$),[7] 60 ($C_{16}TAB$).[3] [c] Assuming that the solubility in the core is equal to that in a hydrocarbon solvent. [d] Reference 21. [e] Reference 22. [f] Reference 23. [g] Reference 24. [h] Reference 25. [i] Reference 26.

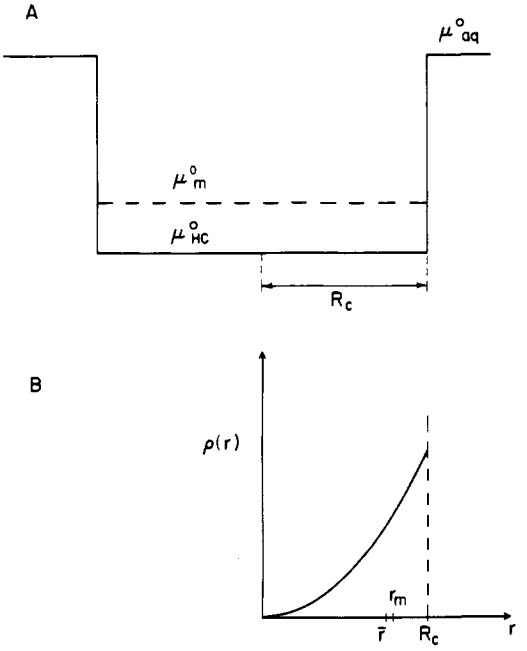

Figure 12. (A) Free-energy well for a solubilized molecule in a micelle regarded as a spherical oil droplet. The standard free energy μ°_{HC} of the molecule in the hydrocarbon solvent is lower than that in the spherical micelle hydrocarbon owing to the Laplacian pressure in the micelle and entropy factors resulting from restrictions on the freedom of motion of the probes. (B) The probability $\rho(r)dr$ of finding the probe between r and $r + dr$ in a spherical well as in (A) depends parabolically on r. The mean distance from the center of the sphere is $\bar{r} = 3R_c/4$, and the median is $r_m = 0.797R_c$.

Table III) for the other arenes, one can estimate the solubility of 4-bromo-*p*-terphenyl to be $<10^{-9}$ M. This would then give a K_{eq} of $>6 \times 10^6$ M^{-1}.

Discussion

The results from the present study of the kinetics of solubilization, solubilities in micellar solutions, and distribution of probe molecules between micelles and the aqueous phase will be discussed with reference to a simple model of solubilization.

Basically, we can regard the micelles as dispersed oil droplets in water.[27] Thermodynamically, these droplets provide a spherical free-energy well for solubilized molecules. We will consider the simplest possible shape of these potential wells that can account for the solubilization phenomena.

From the point of view of solubilization, we regard the micelles as rather static entities in that their number, and essentially also the sizes of the individual micelles, remains unchanged during the average residence time of a solubilized molecule in a micelle. This is in accord with known facts about micelle kinetics. The breakup or formation of a micelle occurs in a time scale of 10–1000 ms[7] whereas the residence time of our probe is of the order of 1–100 μs. On the other hand, a micelle will, on average, lose a monomer in 0.01–10 μs.[7] A number of monomers will thus leave the micelle, and others enter it, during the time that the probe resides in the micelle. It is also known that in some cases minor amounts of additives, like long-chain alcohols, drastically change the slow relaxation process (corresponding to formation or breakdown of micelles), but then in a stabilizing direction. The rate of exchange of monomers, however, appears to be less affected by the presence of an additive.

Let us consider first a spherical droplet of a hydrocarbon solvent with the size of a micelle core. If this drop has the same properties as the bulk solvent, the free-energy potential experienced by a probe would be of the form shown in Figure 12A.

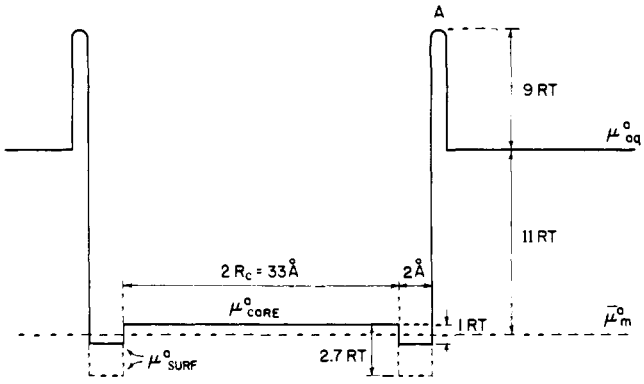

Figure 13. A spherical free-energy well with surface solubilization drawn to represent pyrene in NaLS micelles under the assumption that surface and core solubilization are equally important. The mean standard chemical potential $\bar{\mu}_m^\circ$ of pyrene in the micelle phase is about equal to that in a hydrocarbon solvent according to solubilization measurements. The surface well is assumed to be 2 Å wide. A depth of about RT of the surface well compared to μ°_{core} is then sufficient to place half of the solubilized molecules at the surface. The potential barrier A is a kinetic barrier as estimated in Appendix II. The deeper surface well indicated by the broken line represents the depth required to obtain a solubilization as in $C_{12}AC$.

For a spherical drop this picture should be complemented with Figure 12B, which gives the probability $p(r)dr$ of finding the probe between r and $r + dr$ in the drop. The median distance from the surface in this model is $0.206R_c$. For a drop with the radius of a dodecyl-hydrocarbon chain this amounts to about 3.5 Å from the surface.

The hydrocarbon core of a micelle is not just a hydrocarbon droplet, although predominantly liquid-like in character. There are severe restrictions on the mobilities of the hydrocarbon chains,[28] and thereby also on the different types of motion of a probe.[29] These restrictions will increase the free energy and decrease the solubility of the probe in the hydrocarbon core, and may do so to different extents in different parts of the core. An increased free energy at the center of the core will not be very important—the probe is not likely to be there anyhow—whereas an increase in free energy close to the surface will be very important and decrease the overall solubility substantially.

The micelle surface may also provide sites for solubilization. In fact, for arenes it has been established in some cases that surface solubilization dominates, e.g., benzene,[4,30] toluene,[30] and 2-methylnaphthalene[31] on CTAB. General thermodynamic reasons for aromatic molecules to prefer solubilization at the interface have been given by Mukerjee et al.[4] The surface solubilization should be regarded as a specific effect only if the probe has to overcome a free energy barrier appreciably bigger than $1RT$ when passing from the surface to the interior of the micelle. Such a situation would be expected if the surface solubilization is due to a specific interaction between the probe and the head groups.

Even if there are no specific effects, surface solubilization may still be very important. This is clearly shown by a calculation based on examples in Figure 13. The depth of the surface well has been taken as $1RT$, the hydrocarbon core radius 16.5 Å (approximately the length of a dodecyl chain), and the width of the surface well 2 Å. The latter is somewhat arbitrarily chosen; the width should be of molecular dimensions and reflect the roughness of the micelle surface and the freedom of rotation and radial motion of the probe on the surface. The ratio of surface/core solubilization in this case is 1.1. Furthermore, a probe in the core should spend half the time at a distance of 3.5 Å or shorter from the surface (Figure 12B) and therefore the probe in this case spends ~75% of the time at or close to the surface.

As outlined here the model does not account for interactions between the solutes in the micelle, or changes of the micellar structure due to the presence of the solutes. Clearly, both effects may change the form and the mean depth of the free-energy well. The introduction of solutes into the core will certainly change the volume.

The importance of these factors may be estimated from determinations of the distribution constant at different mean occupancy numbers. The simple model predicts that $K_{eq}/\bar{n}$ (probe concentration in micelles to concentration in the aqueous phase = $\exp\{\Delta G_m^\circ/RT\}$) is a constant independent of the mean occupancy number $\bar{n}$. The type of deviations that may occur at high $\bar{n}$ are illustrated by results from Dougherty and Berg[32] on the distribution of aniline, methyl orthobenzoate (MOB), and 1-fluoro-2,4-dinitrobenzene (FDNB) between water and micelles of NaLS and a dinonylphenylpolyoxyethylene surfactant (DNPE). The distribution constants (the mole fraction ratio x_m/x_{aq}) were determined from very low concentrations up to saturation limits, which in all cases were much higher ($x_m = 0.4$ or more) than for the arenes of the present study. The system FDNB in DNPE behaved ideally; aniline in DNPE gave a maximum distribution constant between $x_m = 0.1$ and 0.2, whereas for MOB in FDNB the distribution constant decreased linearly with x_m. All three solutes in NaLS gave distribution constants that decreased with x_m. For FDNB the decrease was linear over the whole range and rather small: from $K \simeq 1350$ at $x_m = 0$ to $\simeq 1150$ at $x_m = 0.1$. For aniline and MOB the initial decrease was linear and, particularly for aniline, more pronounced.

FDNB is the solute that most resembles the arenes used in the present study—the other two are rather polar and also undergo hydrogen bonding. We note that deviations from ideality for FDNB are quite small. It seems probable that the big deviations, particularly for aniline, to a large extent are due to changes in the nature of the micelles.

For the cases where we have been able to determine the distribution constants both by solubility measurements at the saturation limit and by other methods at low mean occupany numbers, the values are the same within the (rather wide) experimental limits of error (Tables II and III). These cases are naphthalene ($\bar{n}_{max} = 6.2$), 1-bromonaphthalene ($\bar{n}_{max} = 9.4$), 1-methylnaphthalene ($\bar{n}_{max} = \sim 15$), and biphenyl ($\bar{n}_{max} = 3$) in NaLS and also naphthalene in CTAB ($\bar{n}_{max} = 20$).

The approximate constancy of the distribution constant implies a Poisson distribution of the solute among the micelles, as shown in Appendix I. In particular, there is no evidence whatsoever on the strong cooperative effect implicit in Dorrance and Hunter's distribution formula.[33]

The comparison of the solubilities in micelles and hydrocarbon solvents gives some indication of the relative importance of surface solubilization. We can never expect a greater solubility in the hydrcarbon core of a micelle than in a hydrocarbon solvent. In fact we have every reason to expect it to be appreciably lower. Even though 1-methylnaphthalene and 1-bromonaphthalene are both miscible with a hydrocarbon solvent, their maximum solubilities in NaLS micelles are not much bigger than that of naphthalene. One of the major factors affecting the solubility in the micelle core is certainly the Laplacian pressure in the core, $P = 2\gamma/R$ where γ is the interfacial tension and R the micelle radius. Mukerjee[34] has estimated that pressure to be a few hundred atmospheres in micelles like NaLS. This effect alone would decrease the solubility of a probe in the micelle compared to that in a hydrocarbon solvent by a factor of $\exp\{P\bar{V}/RT\}$, where $\bar{V}$ is the molar volume of the probe. At a pressure of 200 atm and with $\bar{V} = 0.1$ L/mol this amounts to a factor of 2.5.

Minimum values of the fraction of surface solubilization can thus be obtained by assigning to the core the solubility of the compound in a hydrocarbon solvent. Such ratios are given in

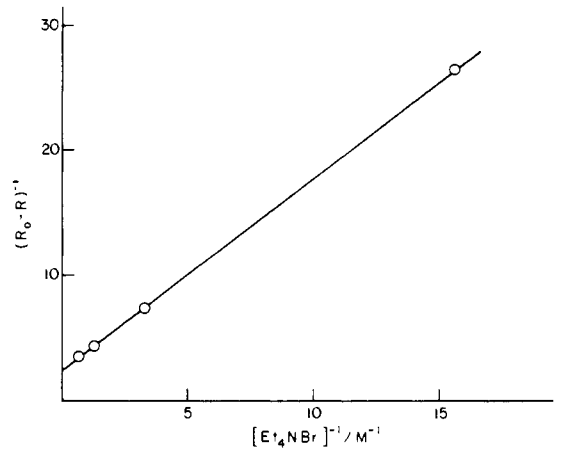

Figure 14. The variation of the pyrene III/I ratio, as a function of the concentrations of tetraethylammonium bromide, plotted in the form given by eq 13. The binding constant of pyrene and Et_4NBr is 1.8 M^{-1}.

Table III from the solubility measurements.

It is apparent from Table III that the solubility increases with the chain length of the surfactant. For the alkyl sulfates the solubility of pyrene seems to level off at the tetradecyl chain length. An increase in core solubility can be understood in terms of increasingly liquid-like properties and a decreased Laplacian pressure of the core as it grows in size.

It seems necessary, though, to also invoke some surface solubilization for the alkyl sulfates. Indeed, already in the case of NaLS the solubility is too high to be explained by exclusive hydrocarbon core solubilization; the solubility should then be appreciably less than that in a hydrocarbon.

The most noticeable feature of Table III is the big difference between the trimethylalkylammonium surfactants (and also dodecylammonium chloride) and the alkyl sulfates with the same chain length. The solubilities in the former are always at least twice as high as in the latter. Pyrene seems to be solubilized predominantly at the surface of these micelles.

It is tempting to invoke a specific interaction between pyrene (and other arenes) and the quaternary ammonium head groups as the reason for the increased surface solubilization. There are some other indications as well. One is the abnormally low ratio between the intensity of the third and first vibronic bands in the fine structure of the pyrene monomer fluorescence spectrum. Kalyanasundaram and Thomas[35] have used this solvent-sensitive ratio to probe the location of pyrene in different micellar systems; NaLS, sodium laurate, and $C_{12}AC$ give ratios of 0.88, 0.96, and 0.95, respectively, as compared to 0.89 in methanol, ~1.67 in hydrocarbons, and 0.63 in water. Trialkylammonium micelles give values in the range 0.79–0.73. We have determined the III/I ratio in ethanol at various concentrations of added tetraethylammonium bromide. The observed change, from 0.89 at 0 and 0.55 at 1.6 M tetraethylammonium bromide, is in accord with the assumptions that a molecular complex is formed with stability constant $\beta = [PQ]/([P]_{tot} - [PQ])\,[Q]$, and that the observed III/I ratio R is the weighted mean value of that of the complex R_c and that of pyrene in ethanol R_0. We then have

$$\frac{1}{R_0 - R} = \frac{1}{R_0 - R_c}\left(1 + \frac{1}{\beta[Q]}\right) \qquad (13)$$

Figure 14 gives a plot according to this equation from which $R_c = 0.47$ and $\beta = 1.8$ M^{-1}. This equilibrium constant evidently represents the excited-state complex, which may be different from that of the ground state.

The stability constant thus found is not particularly large; however, in a micelle of, e.g., CTAB there are about 60 head groups surrounding a volume of only about 10^5 Å^3. This corresponds to 1 mol of head groups per L of hydrocarbon core. Using the above stability constant we find that pyrene should prefer the head groups over the core by a factor of about 2. The justification for this comparison is that the solvent properties of the surface of the micelle in some aspects resemble that of ethanol,[36] and that the solubility of pyrene in ethanol is about the same as in a hydrocarbon.[25] From Table III the minimum surface/core solubilization ratio obtained is 4.5.

In conclusion, the solubility data indicates strongly that pyrene is preferentially solubilized at the surface of alkylammonium-surfactant micelles. A rather weak interaction between the head groups and the arene seems to be the major reason. This conclusion is probably applicable to the other arenes listed in Table III.

In the list of Table III, it can be seen that there are a few molecules which are highly soluble in the micelle, in particular benzene, 1-bromonaphthalene, toluene, and *p*-xylene. For these molecules we have still calculated the distribution constant based on the normal aggregation number and the normal cmc. This may not be completely valid. The high micelle solubility of these compounds will undoubtedly affect the micelle volume and may change the number of surfactant units associated with the micelle. In these cases K_{eq}/N is a better distribution constant, although the uncertainty in the cmc still remains. It is of course just in these cases that a dependence of K_{eq}/N on $\bar{n}$ may be important so that the distribution constant at a low occupancy number may be markedly different.

Kinetic Implications of the Model. With respect to the kinetics of exchange of probe molecules between the micelle and the surrounding aqueous phase, all solubilization sites are equivalent, unless they are surrounded by a high free-energy barrier. The latter might be the case if there is an appreciable barrier to penetrate the surface of the core, or if the surface sites are very deep, due to a strong interaction with the head groups. In both cases the surface solubilization would be expected to be predominant, so that in effect we need only consider the surface sites. The fine structure of the free-energy potential inside the micelle is then not important. In Appendix II we have derived an expression for the rate constants with a free-energy barrier as in Figure 13. For an entirely diffusion-controlled situation the association rate constant would have a value of about $k_+ = (1.2 \pm 0.3) \times 10^{10}$ M^{-1} s^{-1} for NaLS micelles. The result from the study of 1-bromonaphthalene, $k_+ = (5\text{–}8) \times 10^9$ M^{-1} s^{-1}, indicates that the diffusion to the micelle and the final solubilization step are about equally important. The final free-energy barrier would then be $4\text{–}5RT$ higher than the free diffusion barrier of about $4.5RT$, according to Appendix II. The solubility data and distribution constant for 1-bromonaphthalene do not permit an estimation of the extent of surface solubilization—1-bromonaphthalene is miscible with dodecane, so the solubilization might be entirely in the core. (In comparison with the other arenes, though, some surface solubilization would seem likely.) We do not know, therefore, if the free-energy barrier represents the penetration into the core or a barrier before the attachment to the surface. In any case it is quite small, which is to be expected for an initial surface solubilization, where the barrier can be imagined to reflect the search for a suitable spot on the surface among head groups, counterions, and hydration water.

We may assume, therefore, that this barrier, and this association rate constant, is representative for the arenes. The exit rate constants and the residence times of the probes in the micelles are then obtained from the distribution constants and are given in Table IV for NaLS and CTAB. Included are some arenes for which the exit rates have been measured by other techniques.

A means of understanding the trend in the exit rate of the

Table IV. Exit Rates of Aromatic Hydrocarbons from NaLS and CTAB Micelles

arene	equilibrium[a] k_-, s^{-1} NaLS	equilibrium[a] k_-, s^{-1} CTAB	direct k_-, s^{-1} NaLS	direct k_-, s^{-1} CTAB
perylene	4.1×10^2	2.6×10^2		
anthracene	1.7×10^4	3.2×10^3		$\leq 10^3$ [b]
pyrene	4.1×10^3	1.7×10^3		
1-bromonaphthalene	3.3×10^4	4.1×10^3	2.5×10^4	
biphenyl	9.6×10^4	1.6×10^4	1.2×10^5 [c]	
			$>5 \times 10^4$	
1-methynaphthalene	1×10^5		$>5 \times 10^4$	
naphthalene	2.5×10^5		$>5 \times 10^4$	
p-xylene	4.4×10^5			
toluene	1.3×10^6			
benzene	4.4×10^6	7.5×10^5	$\geq 10^4$ [d]	

[a] Calculated using 7×10^9 M^{-1} s^{-1} as the entrance rate. [b] Reference 10. [c] Reference 6. [d] Reference 5; NMR lower limit.

various probes in the two micelle systems can be gained by expressing the exit rate in the form

$$k_- = k_+ \frac{[P]_s}{\bar{n}_{max}} \qquad (14)$$

Although $[P]_s/\bar{n}_{max}$ is used in the above equation, this ratio is approximately constant even for lower probe concentrations; this was mentioned in the previous section. Having k_+ as a constant for the various probes, eq 14 shows that the exit rate, as may be expected, will depend on both the solubility of probe in water and in the micelle. For a particular micelle system, e.g., NaLS data in Table III, it is seen that the solubility in the micelle, $\bar{n}$, does not vary as much as the solubility of the various probes in water. Thus the exit rates approximately parallel the solubilities in water, i.e., the greater the solubility in water, the larger is the exit rate from that particular micelle.

The same behavior in the exit rates is also seen for the CTAB micelles, with the noticeable difference being that the exit rates are from five to eight times slower. This of course is reflected in $\bar{n}_{max}$.

Deviations from the general trend shown for the probes in CTAB and NaLS may be expected if in some cases particular probes form strong complexes with the micelle. The data obtained for arene/CTAB systems indicated that there was some complexation of the probes with the micelle, but since the trend in $\bar{n}$ and k_- is very similar to NaLS it must mean that all the probes complex weakly or approximately to the same degree. Equation 14 also suggests that the exit rate will change if the solubility of the probe in water is altered. This can be achieved by the addition of either electrolytes or nonelectrolytes to the micelle/arene system. In practice, however, it is difficult to assign a change in the exit rate purely to a change in the solubility of the probe in water. This is because relatively large amounts of additives are needed to noticeably change the equilibrium, in which case the micelles themselves are altered and may instead be responsible for the observed effect.

Correlation of the Equilibrium Constants with the Boiling Points of the Arenes. It is useful to correlate the solubility data with an easily obtained property of the arenes. This is shown in Figure 15, where the equilibrium constant log (K_{eq}/N) is plotted as a function of the boiling point of the arenes. The reason for this correlation will not be dealt with here; the graph is primarily presented to be used as a guide in determining other equilibrium ratios which have not been measured. The results for perylene have not been plotted since this compound does not have a true boiling point, but sublimes between 350–400 °C. All the boiling point temperatures have been taken from ref 19.

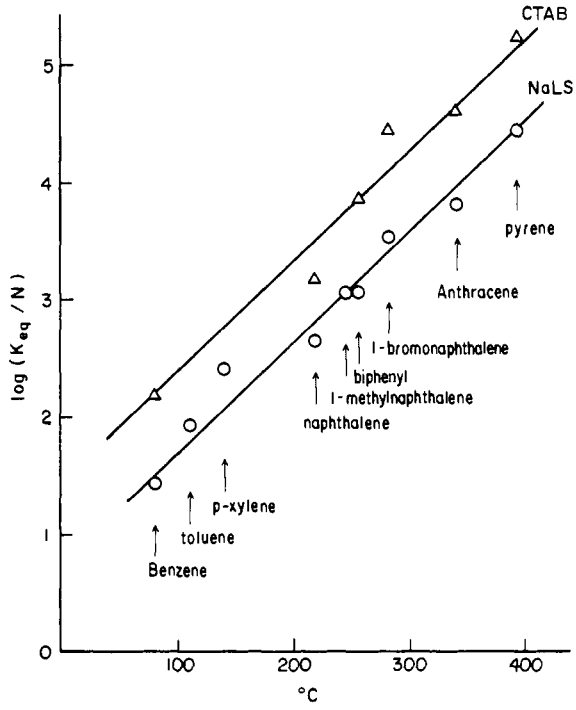

Figure 15. The distribution constant K_{eq}/N of the arenes with NaLS and CTAB plotted as a function of the boiling point of the arenes.

Acknowledgment. M.A. has been supported by grants from the Swedish National Science Research Council. The research described herein was supported by the Office of Basic Energy Research of the Department of Energy.

Appendix I. The Distribution of Solubilized Molecules among Micelles[37]

The statistics for the distribution of solubilized molecules among micelles will in the general case depend on a number of factors; however, it is possible to recognize a simple case which lends itself to a simple mathematical treatment. This is the case when the solubilized molecules neither interact specifically with each other nor perturb the properties of the micelle; in other words, when the presence of solubilized molecules in a micelle neither promotes nor prohibits the solubilization of further molecules.

The distribution is then a Poisson distribution. This is apparent by comparison to a classical example where the latter appears as a limiting case: the formation of a given large number of buns (micelles) from a dough containing a given number of raisins (solubilized molecules). The Poisson distribution has also been used by a number of authors in dealing with, for instance, photochemical processes in micelles.

However, another distribution has been used by Dorrance and Hunter in a series of papers[33] dealing with excimer kinetics of pyrene in CTAB micelles. These authors originally claimed that their relationship was the simplest distribution, following from, essentially, the conditions mentioned above. It was pointed out by Almgren and Aniansson in a note[37] that Dorrance and Hunter had made an error in their statistical derivation, that the correct result should be the Poisson distribution, and, further, that the Poisson distribution follows from a treatment of solubilization as a distribution equilibrium between two phases (and vice versa).

The problem is most conveniently and clearly treated from a kinetic point of view. Solubilization is described by the following equilibria:

$$M + P \underset{k_1^-}{\overset{k_1^+}{\rightleftharpoons}} MP_1$$

$$MP_1 + P \underset{k_2^-}{\overset{k_2^+}{\rightleftharpoons}} MP_2$$

$$MP_{i-1} + P \underset{k_i^-}{\overset{k_i^+}{\rightleftharpoons}} MP_i$$

where MP_i is a micelle containing i solubilized molecules P. The simplest case according to the conditions above is given by

$$k_i^+ = k^+$$
$$k_i^- = ik^- \tag{I-1}$$

when k^+ and k^- are independent of i. At equilibrium

$$\frac{[MP_i]}{[MP_{i-1}]} = \frac{k_+[P]_{aq}}{k_- i} \equiv \frac{K[P]_{aq}}{i} \tag{I-2}$$

Combining equations of this type for $i = 1$ to i, we obtain

$$\frac{[MP_i]}{[M]} = \frac{(K[P]_{aq})^i}{i!} \tag{I-3}$$

Assuming that there is no limit to the number of solubilized molecules per micelle (which in practice means that we restrict the validity to low mean occupancy numbers) we obtain for the mean occupancy

$$\bar{n} \equiv \frac{\sum_{i=0}^{\infty} i[MP_i]}{\sum_{i=0}^{\infty} [MP_i]} = \frac{\sum_{i=0}^{\infty} i\frac{(K[P]_{aq})^i}{i!}}{\sum_{i=0}^{\infty} \frac{(K[P]_{aq})^i}{i!}} = K[P]_{aq} \tag{I-4}$$

The fraction of micelles with i solubilized molecules is then given by

$$P_i \equiv \frac{[MP_i]}{[M]_{tot}} = \frac{\frac{(K[P]_{aq})^i}{i!}}{\sum_{i=0}^{\infty} \frac{(K[P]_{aq})^i}{i!}} = \frac{\bar{n}^i e^{-\bar{n}}}{i!} \tag{I-5}$$

which is the Poisson distribution. Equation I-4 gives us

$$\frac{\bar{n}}{[P]_{aq}} = \frac{[P]_{micelle}}{[P]_{aq}[M]_{tot}} = K \tag{I-6}$$

which is a form of the law of distribution between phases.

It is possible to start with that law and seek the condition on k_i^+/k_i^- that makes it applicable. The condition turns out to be

$$k_i^+/k_i^- = K/i \tag{I-7}$$

where K is independent of i. This condition is somewhat less restrictive than eq I-1, but will still result in eq I-5.

The distribution constant K is experimentally accessible; as long as K is independent of $\bar{n}$, the Poisson distribution should hold. It is of interest to inquire how well such an experimental test would discriminate between the Poisson distribution and the one of Dorrance and Hunter.[33] The latter is given by

$$P_j' = \frac{\bar{n}^j}{(1+\bar{n})^{j+1}} \tag{I-8}$$

Let us denote the experimental distribution constant for $\bar{n} \to 0$ by K_0.

$$K_0 = \lim_{\bar{n}\to 0} K = \frac{k_1^+}{k_1^-} = \frac{[MP]}{[P]_{aq}[M]} = \frac{P_1'}{[P]_{aq}P_0'} \tag{I-9}$$

Insertion of $[P]_{aq}$ from this relation into eq I-6 gives

$$\frac{K}{K_0} = \frac{\bar{n}P_0'}{P_1'} = 1 + \bar{n} \tag{I-10}$$

Thus, this distribution predicts a linear dependence of K on $\bar{n}$; already at $\bar{n} = 1$ the distribution constant would be twice as big as at $\bar{n} \ll 1$. This would be easily observed experimentally.

Appendix II. Exit and Entry Rates

Consider the free-energy barrier in Figure 13. The rate of jumping over the barrier, from one equilibrium position just outside to one just inside, a distance λ away, is given by[38]

$$J_+ = 4\pi R_0^2 \lambda k_0 C(R_+) \tag{II-1}$$

when $C(R_+)$ = concentration just outside the barrier and

$$k_0 = \frac{kT}{h}\exp\left\{\frac{-\Delta G^{\ddagger}}{RT}\right\} \tag{II-2}$$

R_0 is the micelle radius. A steady-state diffusion from a concentration $C(\infty) = [P]_{aq}$ to $C(R_+)$ just outside the micelle gives an inward flow

$$J_+ = 4\pi R_0 D([P]_{aq} - C(R_+)) \tag{II-3}$$

At the steady state, with zero concentration inside the micelle, the flows of eq 1 and 3 must be equal. Eliminating $C(R_+)$ we obtain

$$J_+ = 4\pi R_0 [P]_{aq}\left(\frac{1}{D} + \frac{1}{\lambda R_0 k_0}\right)^{-1} \tag{II-4}$$

This is a well-known result for steady-state diffusion.[39]

Let us now consider the outward flow of probe molecules. The mean equilibrium concentration inside the micelle is given by

$$\bar{C}_m = \frac{3\bar{n}}{4\pi R_0^3} \tag{II-5}$$

where $\bar{n}$ is the mean number of probes per micelle. We will consider jumps from the mean chemical potential in the micelle over the surface barrier. Alternatively, with a more detailed picture we could begin at, say, a lower chemical potential just inside the barrier. However, the concentration there would be correspondingly higher.

For the outward jump rate we have

$$4\pi R_0^2 \lambda \frac{3\bar{n}}{4\lambda R_0^3}\frac{kT}{h}\exp\left\{\frac{\Delta G_m^{\circ}}{RT} - \frac{\Delta G^{\ddagger}}{RT}\right\} \tag{II-6}$$

However, since the concentration just outside the barrier is not zero, we must consider reentry from that position, in addition to the outward diffusion. At the steady state, with concentration $\bar{C}_m$ inside the micelle and $C(\infty) = 0$, we find

$$J_- = \frac{3\bar{n}}{R_0}\lambda k_0 \exp\left\{\frac{\Delta G_m^{\circ}}{RT}\right\} - 4\pi R_0^2 \lambda k_0 C(R_+) = 4\pi R_0 C(R_+) D \tag{II-7}$$

and, eliminating $C(R_+)$

$$J_- = \frac{3\bar{n}}{R_0^2}\exp\left\{\frac{\Delta G_m^{\circ}}{RT}\right\}\left(\frac{1}{D} + \frac{1}{\lambda R_0 k_0}\right)^{-1} \tag{II-8}$$

At equilibrium we have $J_- = J_+$ and thus

$$\frac{\bar{n}/^4/_3\pi R_0^3}{[P]_{aq}} = \exp\left(-\frac{\Delta G_m^{\circ}}{RT}\right) \tag{II-9}$$

as should be expected for a distribution equilibrium. The rate constants used in this study

$$P + MP_{n-1} \underset{nk_-}{\overset{k_+}{\rightleftharpoons}} MP_n$$

are given by

$$k_+ = 4\pi R_0 L \left(\frac{1}{D} + \frac{1}{\lambda R_0 k_0}\right)^{-1} \quad \text{(II-10a)}$$

$$k_- = \frac{3}{R_0^2} \exp\left(\frac{\Delta G_m^\circ}{RT}\right) \left(\frac{1}{D} + \frac{1}{\lambda R_0 k_0}\right)^{-1} \quad \text{(II-10b)}$$

$$K = \frac{k_+}{k_-} = L\frac{4}{3}\pi R_0^3 \exp\left(\frac{\Delta G_m^\circ}{RT}\right) = \bar{V}_m \exp\left(\frac{\Delta G_m^\circ}{RT}\right) \quad \text{(II-11)}$$

where L is Avogadro's number and $\bar{V}_m$ is the molar volume of the micelles.

For the case where the kinetic barrier is low, the rates of the processes are controlled by the diffusion to and from the micelle. Regarding the diffusion process as a succession of jumps over free-energy barriers between adjacent equilibrium positions in the liquid, we have the relationship[38]

$$\frac{D}{\lambda^2} = \frac{kT}{h} \exp\left\{-\frac{\Delta G^{\ddagger}_D}{RT}\right\} \quad \text{(II-12)}$$

where D is the diffusion constant of the probe in water, λ is the jump length, and $\Delta G^{\ddagger}_D$ is the free-energy barrier for diffusion. We should have a diffusion-controlled process if the barrier just outside the micelle is of the same kind as the diffusion barrier in the aqueous solution. This assumption gives $k_0 = D/\lambda^2$; thus $\lambda R_0 k_0 = (R_0/\lambda)D \gg D$, so that (II-10) reduces to

$$\left.\begin{aligned} k_+ &= 4\pi R_0 D L \quad \text{(II-13)} \\ k_- &= \frac{3D}{R_0^2} \exp\left(\frac{\Delta G_m^\circ}{RT}\right) \quad \text{(II-14)} \end{aligned}\right\} \text{(diffusion controlled)}$$

If on the other hand $D \gg \lambda R_0 k_0$ we have

$$\left.\begin{aligned} k_+ &= 4\pi R_0^2 \lambda k_0 L \quad \text{(II-15)} \\ k_- &= \frac{3k_0}{R_0} \exp\left(\frac{\Delta G_m^\circ}{RT}\right) \quad \text{(II-16)} \end{aligned}\right\} \text{("reaction" controlled)}$$

The turnover point between diffusion-controlled and reaction-controlled kinetics may be taken as the case where $D = \lambda R_0 k_0$; k_+ should then be half of the diffusion-controlled value.

An estimate of the diffusion controlled rate from eq II-13 should be quite good in the present case where diffusion of a small molecule to a relatively large sphere is considered. Using $D = (8 \pm 0.2) \times 10^{-5}$ cm^2/s for the diffusion constant in water for the probes studied (benzene, benzenesulfonic acid, and naphthalenesulfonic acid are all in this range[40]) and $R = 20$ Å one obtains

$$k_+ = (1.2 \pm 0.3) \times 10^{10}\ \text{M}^{-1}\ \text{s}^{-1}$$

It is of some interest also to estimate the kinetic free-energy barrier. With D as above, and assuming $\lambda = 1$ Å (it should be of about the molecular dimensions of the solvent[38]), we have $\Delta G^{\ddagger}_D = 4.4RT$. At the turnover point between diffusion-controlled and reaction-controlled kinetics, we have $k_0 = (kT)/n \exp(-\Delta G^{\ddagger})/(RT) = D/(\lambda R_0)$, which gives $\Delta G^{\ddagger} = 9RT$.

It remains to consider if the boundary conditions chosen in the above calculation are appropriate for the phosphorescence quenching studies. The use of a negatively charged quencher with negatively charged micelles ensures that no quenching occurs at the very surface of the micelle.[41] The quenchers are thus repelled from the micelle surface. Further, the highest quencher concentration actually used, 2 mM, corresponds to a situation where a sphere with 60 Å radius, three times the micelle radius, on the average contains just one quencher. The outward diffusion process of the probe should not be appreciably perturbed under those conditions.

References and Notes

(1) P. H. Elworthy, A. T. Florence, and C. B. Macfarlane, "Solubilization by Surface-Active Agents", Chapman and Hall, London, 1968.
(2) M. E. L. McBain and E. Hutchinson, "Solubilization and Related Phenomena", Academic Press, New York, N.Y., 1955.
(3) J. H. Fendler and E. J. Fendler, "Catalysis in Micellar and Macromolecular Systems", Academic Press, New York, N.Y., 1975.
(4) P. Mukerjee, J. R. Cardinal, and N. R. Desai in "Micellization, Solubilization and Microemulsions", Vol. I, K. L. Mitall, Ed., Plenum Press, New York, N.Y., 1977, p 241.
(5) T. Nakagawa and K. Tori, *Kolloid-Z. Z. Polym.*, **194,** 143 (1964).
(6) S. C. Wallace and J. K. Thomas, *Radiat. Res.*, **54,** 49 (1973).
(7) E. A. G. Aniansson, S. N. Wall, M. Almgren, H. Hoffmann, I. Kielmann, W. Ulbricht, R. Zana, J. Lang, and C. Tondre, *J. Phys. Chem.*, **80,** 905 (1976).
(8) Y. Moroi, K. Motomura, and R. Matuura, *J. Colloid Interface Sci.*, **46,** 111 (1974).
(9) K. Kalyanasundaram, F. Grieser, and J. K. Thomas, *Chem. Phys. Lett.*, **51,** 501 (1977).
(10) P. P. Infelta, M. Grätzel, and J. K. Thomas, *J. Phys. Chem.*, **78,** 190 (1974).
(11) N. J. Turro, M. W. Geiger, R. R. Hautala, and N. E. Schore in ref 4.
(12) The technique used to measure the lifetimes (reported in ref 9) of the phosphorescence was subsequently shown to be inaccurate at long emission lifetimes. Measurements using the flash technique described in this report, on similar systems used in ref 9, yielded lifetimes generally in the 1–3-ms time range. Taking extensive precautions in sample preparations, longer lifetimes could be obtained, and the longest of these was 7 ms for biphenyl in NaLS.
(13) F. H. Quina and V. G. Toscano, *J. Phys. Chem.*, **81,** 1750 (1977).
(14) R. R. Hautala, N. E. Schore, and N. J. Turro, *J. Am. Chem. Soc.*, **95,** 5508 (1973).
(15) A. Treinin and E. Hayon, *J. Am. Chem. Soc.*, **98,** 3884 (1976).
(16) The critical micelle concentrations used in this work were obtained from P. Mukerjee and K. J. Mysels, "Critical Micelle Concentrations of Aqueous Surfactant Systems," NSRDS-NBS 36.
(17) (a) F. Reiss-Husson and V. Luzzati, *J. Phys. Chem.*, **68,** 3504 (1964); (b) D. Debye and E. W. Anacker, *J. Phys. Colloid Chem.*, **55,** 644 (1951).
(18) M. S. Fernandez and P. Fromherz, *J. Phys. Chem.*, **81,** 1755 (1977).
(19) "CRC Handbook of Chemistry and Physics", 52nd ed., Chemical Rubber Publishing Co., Cleveland, Ohio.
(20) L. M. Kushner, W. D. Hubbard, and R. A. Parker, *J. Res. Natl. Bur. Stand.*, **59,** 113 (1957).
(21) The solubility may be too large, owing to supersaturation; see text.
(22) J. McKenna, J. M. McKenna, and D. W. Thornthwaite, *J. Chem. Soc., Chem. Commun.*, 809 (1977).
(23) D. MacKay and W. Y. Shin, *J. Chem. Eng. Data*, **22,** 399 (1977).
(24) F. P. Schwarz, *J. Chem. Eng. Data*, **22,** 273 (1977).
(25) A. Seidell, "Solubilities of Organic Compounds", 3rd ed., Van Nostrand, Princeton, N.J., 1942; A. Seidell and W. F. Linke, Supplement to 3rd ed., 1951.
(26) R. L. Bohon and W. F. Claussen, *J. Am. Chem. Soc.*, **73,** 1571 (1951).
(27) These droplets are not quite like a simple hydrocarbon phase since they do possess a number of additional features. However, it is useful for the moment to consider the micelle interior as a true hydrocarbon phase.
(28) (a) E. Williams, B. Sears, A. Allerband, and E. H. Cordes, *J. Am. Chem. Soc.*, **95,** 4871 (1973); (b) A. A. Ribeiro and E. A. Dennis, *J. Phys. Chem.*, **81,** 957 (1977).
(29) (a) M. Grätzel and J. K. Thomas, *J. Am. Chem. Soc.*, **95,** 6885 (1973); (b) K. Kalyanasundaram, M. Grätzel, and J. K. Thomas, *ibid.*, **97,** 3915 (1975).
(30) J. C. Eriksson and G. Gillberg, *Acta Chem. Scand.*, **20,** 2019 (1966).
(31) J. Ulmius, B. Lindman, G. Lindblom, and T. Drakenberg, *J. Colloid Interface Sci.*, **65,** 88 (1978).
(32) S. J. Dougherty and J. C. Berg, *J. Colloid Interface Sci.*, **48,** 110 (1974).
(33) (a) R. C. Dorrance and T. F. Hunter, *J. Chem. Soc., Faraday Trans. 1*, **68,** 1312 (1972); (b) *ibid.*, **70,** 1572 (1974).
(34) P. Mukerjee, private communication.
(35) K. Kalyanasundaram and J. K. Thomas, *J. Am. Chem. Soc.*, **99,** 2039 (1977).
(36) K. Kalyanasundaram and J. K. Thomas, *J. Phys. Chem.*, **81,** 2176 (1977).
(37) Parts of this appendix are taken from an unpublished manuscript by M. Almgren and E. A. G. Aniansson, prepared as a comment to ref 33a but not accepted.
(38) S. Glasstone, K. J. Laidler, and H. Eyring, "The Theory of Rate Processes", McGraw-Hill, New York, N.Y., 1941.
(39) See, e.g., S. H. Lin, K. P. Li, and H. Eyring in "Physical Chemistry", Vol. VII, H. Eyring, D. Henderson, and W. Jost, Ed., Academic Press, New York, N.Y., 1975.
(40) Landolt-Börnstein, "Zahlenwerte und Funktionen aus Physik, Chemie, Astronomie und Technik", Vol. II, Part 5a, Springer-Verlag, West Berlin, 1969.
(41) Efficient surface quenching would be expected to lead to quite different kinetics. Both static quenching and the transient terms in the diffusion of the probe from the interior to the surface would be expected to be important, leading to deviations from simple (quasi-) first-order kinetics.